Limits on different Majoron decay modes of ^{100}Mo and ^{82}Se for neutrinoless double beta decays in the NEMO-3 experiment

R. Arnold [j], C. Augier [h], J. Baker [e], A.S. Barabash [1) g], V. Brudanin [c], A.J. Caffrey [e], E. Caurier [j], V. Egorov [c], K. Errahmane [h], A.I. Etienvre [h], J.L. Guyonnet [j], F. Hubert [a], Ph. Hubert [a], C. Jollet [j], S. Jullian [h], S. King [n], O. Kochetov [c], S. Konovalov [g], V. Kovalenko [c], D. Lalanne [h], F. Leccia [a], C. Longuemare [b], G. Lutter [a], Ch. Marquet [j], F. Mauger [b], F. Nowacki [j], H. Ohsumi [m] F. Piquemal [a], J-L. Reyss [d], R. Saakyan [n], X. Sarazin [h], Yu. Shitov [c], L. Simard [h], F. Šimkovic [o], A. Smolnikov [c], I. Štekl [k], J. Suhonen [f], C.S. Sutton [i], G. Szklarz [h], V. Timkin [c], J. Thomas [n], V. Tretyak [c], V. Umatov [g], L. Vála [k], I. Vanyushin [g], V. Vasilyev [g], V. Vorobel [ℓ], Ts. Vylov [c]

[a] *CENBG, IN2P3-CNRS et Université de Bordeaux, 33170 Gradignan, France*

[b] *LPC, IN2P3-CNRS et Université de Caen, 14032 Caen, France*

[c] *JINR, 141980 Dubna, Russia*

[d] *CFR, CNRS, 91190 Gif sur Yvette, France*

[e] *INL, Idaho Falls, ID 83415, U.S.A.*

[f] *JYVÄSKYLÄ University, 40351 Jyväskylä, Finland*

[g] *ITEP, 117259 Moscow, Russia*

[h] *LAL, IN2P3-CNRS et Université Paris-Sud, 91405 Orsay, France*

[i] *MHC, South Hadley, Massachusetts 01075, U.S.A.*

[j] *IReS, IN2P3-CNRS et Université Louis Pasteur, 67037 Strasbourg, France.*

[k] *IEAP, Czech Technical University, CZ-128 00 Prague, Czech Republic.*

[ℓ] *Charles University, Prague, Czech Republic.*

[m] *SAGA University, Saga, Saga 840-8502, Japan*

[n] *University College London, London, UK*

[o] *FMFI, Comenius University,SK-842 48 Bratislava, Slovakia*

NEMO Collaboration

Preprint submitted to Elsevier Science

Abstract

The NEMO-3 tracking detector is located in the Fréjus Underground Laboratory. It was designed to study double beta decay in a number of different isotopes. Presented here are the experimental half-life limits on the double beta decay process for the isotopes ^{100}Mo and ^{82}Se for different Majoron emission modes and limits on the effective neutrino-Majoron coupling constants. In particular, new limits on "ordinary" Majoron (spectral index 1) decay of ^{100}Mo ($T_{1/2} > 2.7 \cdot 10^{22}$ y) and ^{82}Se ($T_{1/2} > 1.5 \cdot 10^{22}$ y) have been obtained. Corresponding bounds on the Majoron-neutrino coupling constant are $\langle g_{ee} \rangle < (0.4 - 1.9) \cdot 10^{-4}$ and $< (0.66 - 1.7) \cdot 10^{-4}$.

PACS: 23.40.-s, 14.80.Mz

Key words: Majoron, double-beta decay.

[1] Corresponding author, Institute of Theoretical and Experimental Physics, B. Cheremushkinskaya 25, 117259 Moscow, Russia, e-mail: Alexander.Barabash@itep.ru, tel.: 007 (095) 129-94-68, fax: 007 (095) 883-96-01

1 Introduction

Spontaneous violation of global (B-L) symmetry in gauge theories leads to the existence of a massless Goldstone boson, the Majoron. The Majoron, if it exists, could play an important role in Cosmology [1,2,3] and Astrophysics [4,5,6,7]. At the beginning of the 1980's, the singlet [8], doublet [9] and triplet [10] Majoron models were developed. All these models resulted in the neutrinoless double beta decay with the emission of a Majoron

$$(A, Z) \rightarrow (A, Z + 2) + 2e^- + \chi^0 \tag{1}$$

However, the interaction of the triplet (or doublet) Majorons with the Z^0 boson would give a contribution to the width of the Z^0 decay, which corresponds to two (or 1/2) additional massless neutrino types (see for example [11,12,13]). LEP data gives 2.994 ± 0.012 neutrino types [14], thus the triplet and some doublet Majorons are excluded. On the other hand the singlet "see-saw" Majoron [8] is extremely weakly coupled with neutrinos. Nevertheless, in reference [15] it is proposed that a small gauge coupling constant (which determines the Majoron coupling to the Z^0 boson) does not eliminate the possibility of a large Yukawa coupling of Majoron to neutrinos. Thus, the singlet or dominantly singlet Majorons can still contribute to neutrinoless 2β decay [15,16].

Another possibility for neutrinoless 2β-decay with Majoron emission arises in supersymmetric models with R-parity violation [16,17]. Mohapatra and Takasugi [17] proposed that there could be $2\beta\chi^0\chi^0$-decay with the emission of two Majorons :

$$(A, Z) \rightarrow (A, Z + 2) + 2e^- + 2\chi^0 \tag{2}$$

In the 1990's several new "Majoron" models were suggested. The term "Majoron" here denotes massless or light bosons with a coupling to neutrinos. In these models the "Majoron" can carry a lepton charge, but cannot be a Goldstone boson [19]. Additionally there can be decays with the emission of two "Majorons" [20]. In the models with a vector "Majoron", the Majoron is the longitudinal component of the massive gauge boson emitted in 2β decay [21]. All these new objects are called Majorons for simplicity. The possibility for 2β decay with the emission of one or two Majorons was discussed also in the framework of the $SU(3)_L \otimes SU(1)_N$ electroweak model [18].

Recently a new "economical" model for neutrino mass was proposed in the context of the brane-bulk scenarios for particle physics. In this model the standard global B-L symmetry is broken spontaneously by a gauge singlet

Higgs field in the bulk. This leads to a bulk singlet Majoron whose Kaluza-Klein excitations may make it visible in neutrinoless double beta decay [22].

In Table 1 there are 10 Majoron models presented (following [20,21,22,23]), which are considered in this paper. It is divided into two sections, one for lepton number violating (I) and one for lepton number conserving models (II). The last line corresponds to the bulk majoron model. The table also shows whether the corresponding 2β decay is accompanied by the emission of one or two Majorons. The next three entries list the main features of the models: the third column lists whether the Majoron is a Goldstone boson or not (or a gauge boson in the case of vector Majorons, type IIF, or a bulk field Majoron). In column four the leptonic charge L is given. Column five gives the "spectral index" n of the summed energy of the emitted electrons, which is defined by the phase space of the emitted particles, $G \sim (Q_{\beta\beta} - T)^n$. Here $Q_{\beta\beta}$ is the energy released in the decay and T the energy of the two electrons. The energy spectra of different modes of $2\beta 2\nu$ ($n = 5$), $2\beta\chi^0$ ($n = 1, 2$ and 3) and $2\beta\chi^0\chi^0$ ($n = 3$ and 7) decays are presented in Fig 1. The different shapes can be used to distinguish the different Majoron decay modes from each other and 2β-decay with the emission of two neutrinos. In the last column of Table 1 the nuclear matrix elements (NME) are listed.

Attempts to observe 2β decay with Majoron emission have been carried out for the past 20 years. Consequently there now exist strong limits on the "ordinary" Majoron with the "standard" electron energy spectrum shape ($n = 1$), see Table 2. Sufficiently less information exists for "non-ordinary" Majoron models. The most carefully studied "non-ordinary" models are being investigated in [39] for ^{76}Ge, and in [40] for ^{100}Mo, ^{116}Cd, ^{82}Se and ^{96}Zr (see also [34] for ^{116}Cd).

In this paper a systematic search for 2β-decays with different Majoron types is described for ^{100}Mo and ^{82}Se, using the experimental data obtained with the NEMO-3 detector. The first results from NEMO-3 were published in [41,42,43].

2 NEMO-3 detector

A schematic of the NEMO-3 detector is shown in (Fig. 2). The main goal of the NEMO-3 experiment is to study neutrinoless double beta decay of different isotopes (^{100}Mo, ^{82}Se etc.) with a sensitivity of up to $\sim 10^{25}$ y, which corresponds to a sensitivity to the effective Majorana neutrino mass at the level of $\sim (0.1 - 0.3)$ eV [44]. The planned sensitivity to double beta decay with Majoron emission is $\sim 10^{23}$ y (the sensitivity to the coupling constant of the Majoron to the neutrino $< g_{ee} >$ is $\sim n \cdot 10^{-5}$). In addition, one of the goals

is a precise study of $2\beta2\nu$ decay for a number of nuclei (^{100}Mo, ^{82}Se, ^{116}Cd, ^{150}Nd, ^{130}Te, ^{96}Zr and ^{48}Ca) with high statistics to study all characteristics of the decay.

NEMO-3 is a tracking detector, which in contrast to ^{76}Ge experiments [45,46], detects not only the total energy deposition but also the path and energy of the individual electrons. This also provides a unique opportunity to monitor and reject the background. Since June 2002 NEMO-3 has been running in the Fréjus Underground Laboratory (France) located at a depth of 4800 m w.e.

The detector has a cylindrical shape and consists of 20 identical sectors (see Fig 2). A thin ($\sim$30-60 mg/cm^2) source foil placed in the center of the detector contains 2β decaying nuclei and has a total area of 20 m^2 and a weight of about 10 kg. In particular, it includes 7.1 kg of enriched Mo (average enrichment 98%, the total mass of ^{100}Mo is 6.914 kg) and 0.96 kg of Se (enrichment 97%, the total mass of ^{82}Se is 0.932 kg). To investigate the external background the part of the source are made of very pure natural material (TeO_2 -767 g and Cu - 621 g). The contamination of the sources with radioactive impurities was obtained from measurements using low-background HPGe-detectors.

The basic detection principles are the following: the energy of electrons is measured by plastic scintillators coupled to PMTs (1940 individual counters), while the tracks are reconstructed from the information obtained from the Geiger cells (6180 cells). The tracking volume of the detector is filled with a mixture consisting of 95% He, 4% alcohol, 1% Ar and 0.15% water at slightly above atmospheric pressure. In addition, a magnetic field of 25 Gauss parallel to the detector axis is created by a solenoid surrounding the detector. The magnetic field is used to identify electron-positron pairs and to suppress the background associated with these events.

The main characteristics of the detector's performance are the following: the energy resolution of the scintillation counters lies in the interval of 14-17% (FWHM for 1 MeV electrons); the time resolution is 250 ps for an electron energy of 1 MeV; the reconstruction accuracy of a $2e^-$ vertex is approximately 1 cm. The characteristics of the detector are determined in special calibration measurements with radioactive sources. The energy calibration is carried out using ^{207}Bi sources (conversion electrons with energies 0.482 and 0.976 MeV) and ^{90}Sr (the end-point of the β spectrum is 2.283 MeV). The vertex reconstruction accuracy for $2e^-$ events are determined by measurements with ^{207}Bi, while the timing properties were determined in measurements with ^{60}Co (two γs emitted simultaneously), ^{207}Bi (two electrons emitted simultaneously) and neutron sources (providing high energy electrons crossing the detector volume).

The detector is surrounded by passive shielding made of 20 cm of steel, 30 cm

of water in tanks around the detector and wood and paraffin at the top and bottom of the detector. The level of radioactive impurities in the construction materials of the detector and of the passive shielding was measured with low-background HPGe detectors.

A full description of the detector and its characteristics can be found in [47].

3 Experimental data

3.1 ^{100}Mo

In this paper, the analysis of 8023 hours of NEMO 3 data is presented. 2e events with a common vertex inside the source were selected. An electron was defined as a track between the source foil and a fired counter with the energy deposited being greater than 200 keV. The track curvature had to be consistent with a negatively charged particle; the time-of-flight measurement had to be consistent with the hypothesis of the two electrons leaving the source from a common vertex simultaneously. In order to suppress the ^{214}Bi background, which is followed by the ^{214}Po α-decay, it was required that there were no delayed Geiger cell hits (with a delay of up to 700 μs) close to the event vertex or the electron track. A typical 2e-event is shown in Fig 3.

Fig 4 (top) shows the $2\beta2\nu$ experimental energy spectrum and result of Monte Carlo (MC) simulations for ^{100}Mo. The total number of useful events (after background subtraction) is $\sim$158000. The signal-to-background ratio is 40:1, while, for energies above 1 MeV it is 100:1. This means that the background is negligibly small. The detection efficiencies which included the selection cuts were estimated for the single state dominance mechanism [48,49] by MC simulations. The detection efficiency calculated by MC was 4.41%. Correspondingly, the following results were obtained for the ^{100}Mo half-life:

$$T_{1/2} = [7.41 \pm 0.02(stat) \pm 0.43(syst)] \cdot 10^{18}\ y$$

3.2 ^{82}Se

The same 8023 h of data were analyzed. The experimental energy spectrum and result of MC simulations of $2\beta2\nu$ events for ^{82}Se are shown in Fig 4 (bottom). The total number of useful events after the background subtraction

was $\sim$ 2020. The signal-to-background ratio was about 4:1. The detection efficiency was calculated by Monte Carlo to be 4.46%. The ^{82}Se half-life value obtained is:

$$T_{1/2} = [9.6 \pm 0.24(stat)^{+0.67}_{-0.59}(syst)] \cdot 10^{19} y.$$

This value is in agreement with the previous measurement made with the NEMO-2 detector [50].

4 Analysis of the Experimental Data

The experimental data for ^{100}Mo and ^{82}Se are shown in Fig. 4. One can see that experimental data are in a good agreement with the MC simulations. Exception is a low energy part of the ^{100}Mo spectrum (0.4-0.8 MeV), where the experimental points are systematically higher than the MC simulations. It can be associated with some physical effect (Majoron decay with $n = 7$ or second-forbidden corrections contribution [51], for example) or with our not ideal knowledge of the response function of the detector. To be conservative now we prefer to be in framework of the last assumption.

The detection efficiencies for the decays depend on the energy of the electrons and were calculated for the two nuclei, for all the Majoron modes (spectral indices $n = 1, 2, 3$ and 7) and for the double beta-decay ($n = 5$) by a Monte-Carlo simulation with the GEANT 3.21 code.

If the Majoron modes are considered as existing decay channels similar to $2\beta2\nu$, then the data contains the sum of two processes, $2\beta2\nu$ decay and the decay with χ^0 emission. Therefore it is not possible to know the expected number of $2\beta2\nu$ decays and so a limit must be set on the decays with Majoron emission by analyzing the deviation in the shape of the energy distribution of the experimental data in comparison with calculated spectrum for $2\beta2\nu$ decay. This can be done with a maximum likelihood analysis.

The experimental spectrum was treated as a histogram. One then needs to take into account that the distribution of the events in each bin is a Poisson one and independent of the others. Thus, one constructs the likelihood function as:

$$\mathrm{L}(\mathrm{N}_\beta, \mathrm{N}_\chi) = \prod_{\mathrm{i}=\mathrm{n}_1}^{\mathrm{n}_2} \frac{e^{-(\mathrm{N}_\beta \eta_{\beta\ \mathrm{i}} + \mathrm{N}_\chi \eta_{\chi\ \mathrm{i}} + \mathrm{N}_{\mathrm{bgr\ i}})}}{\mathrm{N}_{\mathrm{exp\ i}}!} (\mathrm{N}_\beta \eta_{\beta\ \mathrm{i}} + \mathrm{N}_\chi \eta_{\chi\ \mathrm{i}} + \mathrm{N}_{\mathrm{bgr\ i}})^{\mathrm{N}_{\mathrm{exp\ i}}} \quad (3)$$

where n_1 and n_2 are the bin numbers of the energy interval, $N_{exp\ i}$ is the number of experimental events in the i-th bin, $N_{bgr\ i}$ is the expected number of background events, and $\eta_{\beta\ i}$ and $\eta_{\chi\ i}$ are the Monte-Carlo simulated efficiencies of $2\beta2\nu$ and Majoron decays in the i-th bin. Finally, N_β and N_{χ^0} are the average numbers of decays for $2\beta2\nu$ and Majoran decay respectively, and are considered as free parameters.

To find the confidence level for the upper limit on the mean number of decays with Majoron emission ($N_{\chi up}$) the likelihood function (3) has to be normalized and then integrated over all possible values of N_β and N_χ from 0 to $N_{\chi up}$:

$$CL(N_{\chi up}) = \frac{\int_0^{N_{\chi up}} dN_\chi \int_0^\infty dN_\beta\, L(N_\beta, N_\chi)}{\int_0^\infty dN_\chi \int_0^\infty dN_\beta\, L(N_\beta, N_\chi)} \tag{4}$$

where $N_{\chi up}$ is a free parameter while $CL(N_{\chi up})$ is fixed.

5 Results and Discussion.

The half-life limits for ^{100}Mo and ^{82}Se for the different decay modes are presented in Table 3. For ^{100}Mo the limit on decays with $n = 1$ and $n = 2$ obtained here is ~ 5 and ~ 50 times higher than that in [52] and [53], with $n = 3$ approximately 2 orders of magnitude higher than that reported in [40], and the limit on decays with $n = 7$ is improved only by a factor of ~ 1.5. In fact, in the latter case there are extra events in the low energy part of the spectrum and a conservative approach leads to a weak limit on the half-life of this decay. The result for $n = 2$ is approximately 5 times better than estimated in [53] while the ^{82}Se results for n=1, 2 and 3 are improved over the ealier limits [40,53] by $\sim 5 - 6$ times, and the limit for $n = 7$ is improved by ~ 50 times. Using the half-lives one can get limits on the coupling constants for different Majoron models via the relations (5) and (6).

$$T_{1/2}^{-1} = |\langle g_{ee}\rangle|^2 |M|^2 G \text{ for } 2\beta\chi^0, \tag{5}$$

$$T_{1/2}^{-1} = |\langle g_{ee}\rangle|^4 |M|^2 G \text{ for } 2\beta\chi^0\chi^0, \tag{6}$$

The relevant matrix elements M and values of the phase space factors G are presented in Tables 4 and 5. Using the data from Table 3 the limits on the coupling constants are calculated and presented in Table 6.

The summary of the best limits on the coupling constant of the Majoron to neutrinos for ordinary Majorons with n = 1 are presented in Table 2. One of the problems is the uncertainty in the Nuclear Matrix Element (NME) calculations which lead to a dispersion of the $\langle g_{ee} \rangle$ value. In the 3^{rd} column, limits obtained using QRPA (different models) NME from [27,28,29] are presented. Exceptions are ^{48}Ca where Shell Model calculations have been used [24,25] and ^{150}Nd for which NME values were taken from [26] where a Pseudo-SU(3) model taking into account the deformation of the ^{150}Nd nuclei was applied and from [27] were calculations in the framework of QRPA were done (though such an approach is not really correct for deformed nuclei).

In the 4^{th} column of Table 2, limits using the NME from [30] are shown where the RQRPA model was used. In this recent work the suppression effect of higher order terms of the nucleon current have been taken into account and the g_{pp} values were extracted from $2\beta 2\nu$ experiments. The authors analyzed practically all the previous QRPA and RQRPA calculations and concluded that their last calculations give the most reliable and accurate values for NME [†]. If this is indeed the correct approach to the determination of g_{pp} then the best present limit is obtained from our measurements with ^{82}Se and ^{100}Mo: $\langle g_{ee} \rangle < (1.2 - 1.9) \cdot 10^{-4}$ and $\langle g_{ee} \rangle < (1.6 - 1.8) \cdot 10^{-4}$ respectively. If, however, the former approach is taken, and the NME values from [27,28,29] are used, the best limit is obtained from the measurement of $^{100}\mathrm{Mo} : \langle g_{ee} \rangle < (0.4 - 0.7) \cdot 10^{-4}$. One can see from the Table 2 that new the approach leads to more conservative limits on the $\langle g_{ee} \rangle$ coupling constant for all nuclei.

All limits in Table 2 were obtained using phase space factors calculated in [54]. These values are $\sim 20\%$ lower than values obtained from [27] and the limits are therefore conservative and could be a further 10% more sensitive.

To summarize briefly all the experimental results and taking into account uncertainties in NME calculations, the conservative limit on $\langle g_{ee} \rangle$ from double beta decay experiments ("ordinary" Majoron) is at the level $< 2 \cdot 10^{-4}$. It is interesting to note that the Majoron-neutrino coupling constant in the range $4 \cdot 10^{-7} < \langle g_{ee} \rangle < 0.2 \cdot 10^{-4}$ is excluded by the observation of SN 1987A [4,7]. This means that the possible range $2 \cdot 10^{-5} < \langle g_{ee} \rangle < 2 \cdot 10^{-4}$ is still allowed in contrast to conclusions from [4,7] where an overly optimistic limit ($< 3 \cdot 10^{-5}$) from double beta decay experiments was used.

For "non-ordinary" Majoron models, our new limits on $\langle g_{ee} \rangle$ are a few times better than reported in [39,40,34]. Analysis of the results documented above shows that the best limits on the coupling constant for decays with Majoron emission ($n = 3$) were obtained in the measurement of ^{100}Mo and for $n = 7$

[†] This is not related to the ^{150}Nd result, which is presented in [30] just for illustration owing to its deformed nuclear shape

in the measurement of ^{82}Se. For the decay with $n = 2$ limit on string scale M can be established at the level of $M > 1$ TeV (see [22]).

6 Conclusion

Improved limits on different Majoron decay modes of ^{100}Mo and ^{82}Se have been obtained. The most stringent limits on the Majoron to neutrino coupling constants have been established. Data collection is continuing and the sensitivity of the NEMO 3 experiment will be increased in the next five years. In particular, we hope to improve our knowledge of detector response function and clarify the situation with the low energy portion of ^{100}Mo spectrum. Of course, a much better sensitivity ($\sim 10^{-5}$ for "ordinary" Majoron) will be reached in the next generation double beta decay experiments (see, for example, review [53]).

Acknowledgement

The authors would like to thank the Modane Underground Laboratory staff for their technical assistance in running the experiment. Portions of this work were supported by a grant from INTAS (no 03051-3431), a NATO grant (PST CLG 980022) and grant from Grant Agency of the Czech Republic (202/05/P239).

References

[1] V. Berezinsky and J.W.F. Valle, Phys. Lett. B 318 (1993) 360.

[2] A.D. Dolgov and F. Takahashi, Nucl. Phys. B 688 (2004) 189.

[3] D. Kazanas et al., Phys. Rev. D 70 (2004) 033015.

[4] K. Kachelriess, R. Tomas and J.W.F. Valle, Phys. Rev. D 62 (2000) 023004.

[5] R. Tomas, H. Pas and J.W.F. Valle, Phys. Rev. D 64 (2001) 095005.

[6] S. Hannestad, P. Keranen and F. Sannino, Phys. Rev. D 66 (2002) 045002.

[7] Y. Farzan, Phys, Rev. D 67 (2003) 073015.

[8] Y. Chikashige, R.N. Mohapatra, R.D. Peccei, Phys. Rev. Lett. 45 (1980) 1926; Phys. Lett. B 98 (1981) 265.

[9] C. Aulakh, R. Mohapatra, Phys. Lett. B 119 (1982) 136.

[10] G. Gelmini, M. Roncadelli, Phys. Lett. B 99 (1981) 1411.

[11] H.M. Georgi, S.L. Glashow, S. Nussinov, Nucl. Phys. B 193 (1981) 297.

[12] V. Barger et al., Phys. Rev. D 26 (1982) 218.

[13] N.G. Deshpande, Proc. Conf. on Neutrino Masses and Neutrino Astrophysics, ed. V. Barger et al., (Singapore: World Scientific), 1987, p.78.

[14] C. Caso et al. (Particle Data Group), European Physical Journal C 3 (1998) 1.

[15] Z.G. Berezhiani, A.Yu. Smirnov, J.W.F. Valle, Phys.Lett. B 291 (1992) 99.

[16] R.N. Mohapatra, P.B. Pal. Massive Neutrinos in Physics and Astrophysics, (Singapore: World Scientific), 1991.

[17] R.N. Mohapatra, E. Takasugi, Phys. Lett. B 211 (1988) 192.

[18] J.C. Montero, C.A. de S. Pires and V. Pleitez, Phys. Rev. D 64 (2001) 096001.

[19] C.P. Burgess, J.M. Cline, Phys. Lett. B 298 (1993) 141; Phys. Rev. D49 (1994) 5925.

[20] P. Bamert, C.P. Burgess, R.N. Mohapatra, Nucl. Phys. B 449 (1995) 25.

[21] C.D. Carone, Phys. Lett. B 308 (1993) 85.

[22] R. N. Mohapatra, A. Perez-Lorenzana and C.A. de S. Pires, Phys. Lett. B 491 (2000) 143.

[23] M. Hirsch et al., Phys. Lett. B 372 (1996) 8.

[24] J. Retamosa, E. Caurier and F. Nowacki, Phys. Rev. C 51 (1995) 371.

[25] E. Caurier et al., Nucl. Phys. A 654 (1999) 973c.

[26] J.G. Hirsch, O. Castanos and P.O. Hess, Nucl. Phys. A 582 (1995) 124.

[27] F. Simkovic et al., Phys. Rev. C 60 (1999) 055502.

[28] S. Stoica and H.V. Klapdor-Kleingrothaus, Nucl. Phys. A 694 (2001) 269.

[29] O. Civitarese and J. Suhonen, Nucl. Phys. A 729 (2003) 867.

[30] V.A. Rodin et al., nucl-th/0503063.

[31] A.S. Barabash, Phys. Lett. B 216 (1989) 257.

[32] H.V. Klapdor-Kleingrothaus et al., Eur. Phys. J. A 12 (2001) 147.

[33] R. Arnold et al., Nucl. Phys. A 658 (1999) 299.

[34] F. A. Danevich, Phys. Rev. C68 (2003) 035501.

[35] O.K. Manuel, J. Phys. G 17 (1991) 221.

[36] C. Arnaboldi et al., Phys. Lett. B 557 (2003) 167.

[37] R. Luescher et al., Phys. Lett. B 434 (1998) 407.

[38] A. De Silva, M.K. Moe, M.A. Nelson, M.A. Vient, Phys. Rev. C 56 (1997) 2451

[39] M. Gunther et al., Phys. Rev. D 54 (1996) 3641; J. Helmig et al., in : Proc. Int. Worksh. “Bouble beta decay and Related TOpics”, World Scientific, 1996, p.130.

[40] R. Arnold et al., Nucl. Phys. A678, (2000) 141.

[41] R. Arnold et al., JETP Lett. 80, (2004) 377

[42] A. Barabassh et NEMO collaboration, Nucl. Phys. B (Proc. Suppl.) 138, (2005) 207

[43] X. Sarazin et NEMO collaboration, Nucl. Phys. B (Proc. Suppl.) 143, (2005) 221

[44] NEMO-3 Proposal, LAL preprint 94-29 (1994).

[45] H. V. Klapdor-Kleingrothaus et al., Eur. Phys. J. A12, (2001) 147

[46] C. E. Aalseth et al., Phys. Rev. D65 (2002) 092007.

[47] R. Arnold et al., Nucl. Instr. Meth. A536, (2005) 79.

[48] F. Simkovic, P. Domin and S. Semenov, J. Phys. G 27 (2001) 2233.

[49] P. Domin et al., et al., Nucl. Phys. A 753 (2005) 337.

[50] R. Arnold et al., Nucl. Phys. A 636 (1998) 209.

[51] C. Barbero et al., Phys. Lett. B 445 (1999) 249.

[52] K. Fushimi et al., Phys. Lett. B 531 (2002) 190.

[53] A.S. Barabash, Phys. At. Nucl. 67 (2004) 438.

[54] J. Suhonen and O. Civitarese, Phys. Rep. 300 (1998) 123.

[55] C. Barbero et al., Phys. Lett. B 392 (1997) 419.

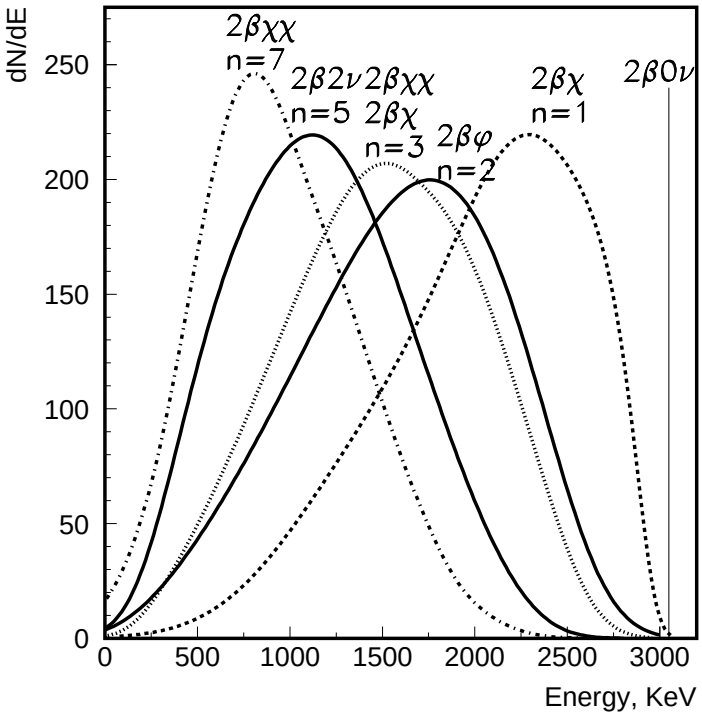

Fig. 1. Energy spectra of different modes of $2\beta 2\nu$ ($n = 5$), $2\beta\chi^0$ ($n = 1$, 2 and 3) and $2\beta\chi^0\chi^0$($n = 3$ and 7) decays of ^{100}Mo.

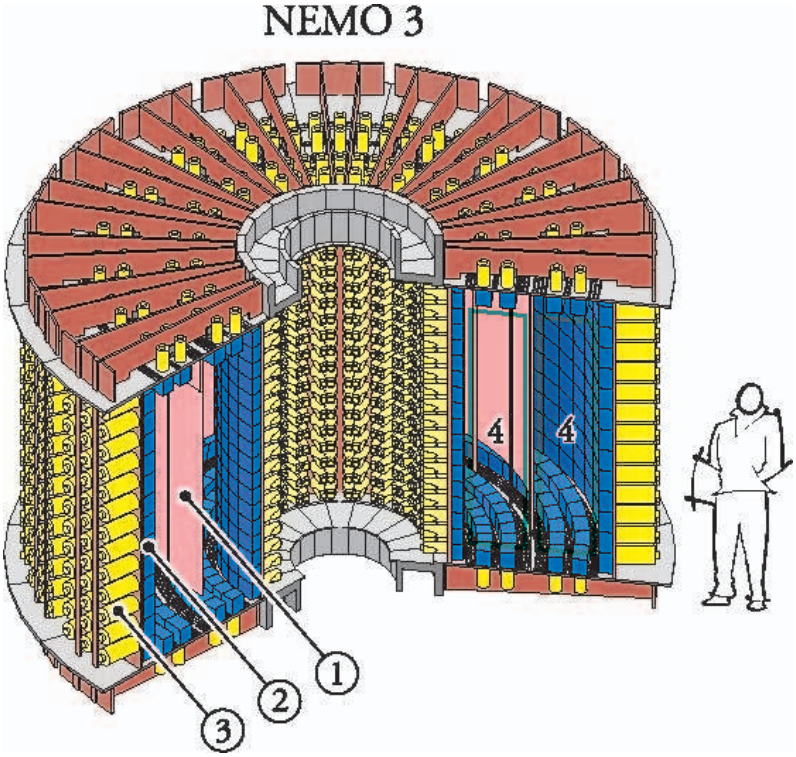

Fig. 2. The NEMO-3 detector without shielding. 1 – source foil; 2– plastic scintillator; 3 – low radioactivity PMT; 4 – tracking chamber.

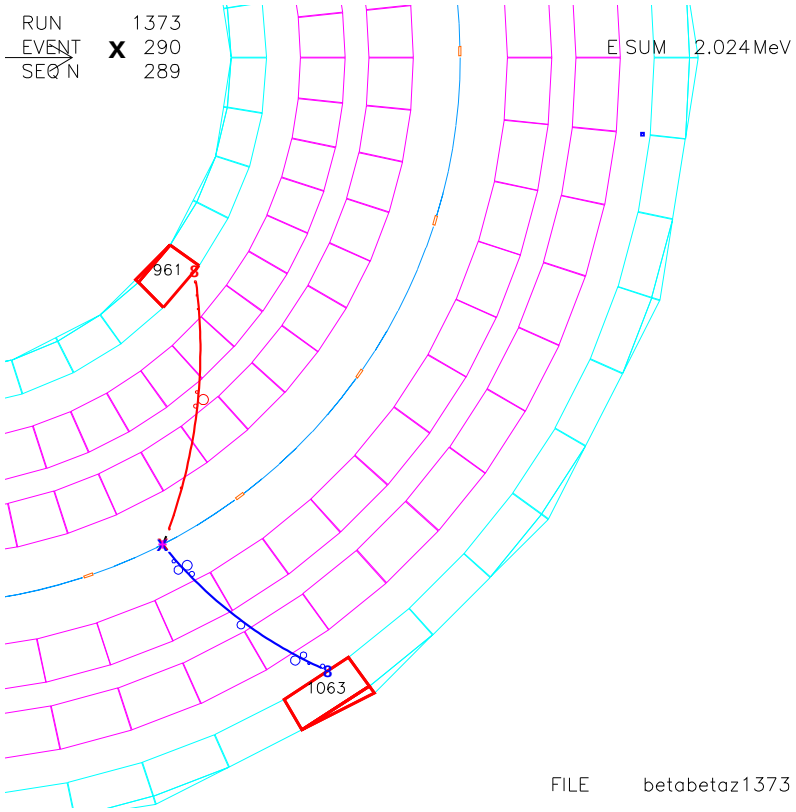

Fig. 3. A view of a reconstructed 2e event in NEMO-3. The sum energy of the electrons is 2024 keV; the energies of the electrons in the pair are 961 keV and 1063 keV.

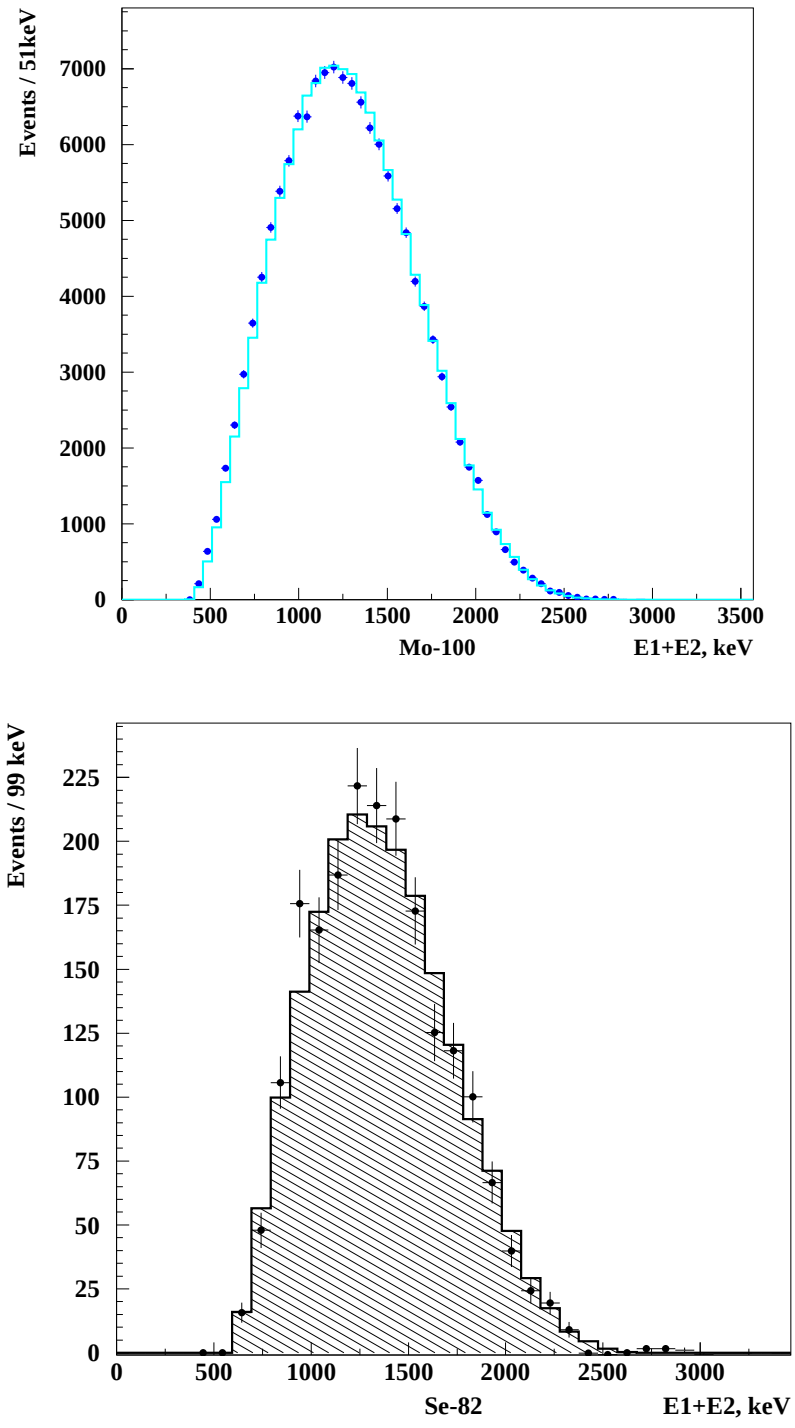

Fig. 4. The 2e events (points - experiment; solid lines - Monte Carlo simulations for $2\beta2\nu$ decay) for ^{100}Mo and ^{82}Se.

Table 1

Different Majoron models according to [20,23]. The mode IIF and "bulk" correspond to the model [21] and [22] respectively.

Case	Decay mode	Goldstone boson	L	n	Matrix element
IB	$2\beta\chi^0$	no	0	1	$M_F - M_{GT}$
IC	$2\beta\chi^0$	yes	0	1	$M_F - M_{GT}$
ID	$2\beta\chi^0\chi^0$	no	0	3	$M_{F\omega^2} - M_{GT\omega^2}$
IE	$2\beta\chi^0\chi^0$	yes	0	3	$M_{F\omega^2} - M_{GT\omega^2}$
IIB	$2\beta\chi^0$	no	-2	1	$M_F - M_{GT}$
IIC	$2\beta\chi^0$	yes	-2	3	M_{CR}
IID	$2\beta\chi^0\chi^0$	no	-1	3	$M_{F\omega^2} - M_{GT\omega^2}$
IIE	$2\beta\chi^0\chi^0$	yes	-1	7	$M_{F\omega^2} - M_{GT\omega^2}$
IIF	$2\beta\chi^0$	gauge boson	-2	3	M_{CR}
"bulk"	$2\beta\chi^0$	bulk field	0	2	–

Table 2

Summary of the best results on the $2\beta\chi^0$ decay with $n = 1$. All limits are presented at the 90% CL. The dispersion of $\langle g_{ee} \rangle$ values is due to uncertainties in the NME calculation. The NME from the following works were used, 3^{rd} column: ^{48}Ca - [24,25], ^{150}Nd - [27,26], and others - [27,28,29]; 4^{th} column: [30].

Nucleus	$T_{1/2}$, y	$\langle g_{ee} \rangle \cdot 10^4$	
^{48}Ca	$> 7.2 \cdot 10^{20}$ [31]	< 12	
^{76}Ge	$> 6.4 \cdot 10^{22}$ [32]	$< (1.2 - 3.0)$	$< (1.9 - 2.3)$
^{82}Se	$> 1.5 \cdot 10^{22}$	$< (0.66 - 1.4)$	$< (1.2 - 1.9)$
	(this work)		
^{96}Zr	$> 3.5 \cdot 10^{20}$ [33]	$< (3.6 - 10)$	$< (35 - 378)$
^{100}Mo	$> 2.7 \cdot 10^{22}$	$< (0.4 - 0.7)$	$< (1.7 - 1.8)$
	(this work)		
^{116}Cd	$> 8 \cdot 10^{21}$ [34]	$< (1.0 - 2.0)$	$< (2.8 - 3.3)$
^{128}Te	$> 2 \cdot 10^{24}$ (geochemical)[35]	$< (0.7 - 1.6)$	$< (1.9 - 2.4)$
^{130}Te	$> 3.1 \cdot 10^{21}$[36]	$< (1.5 - 4.1)$	$< (4.7 - 5.7)$
^{136}Xe	$> 7.2 \cdot 10^{21}$ [37]	$< (1.0 - 7.4)$	$< (5.1 - 6.6)$
^{150}Ne	$> 2.8 \cdot 10^{20}$ [38]	$< (2.5 - 5.5)$	$< (3.8 - 4.8)$

Table 3

Limits on $T_{1/2}$ at 90% CL for decays with Majoron emission, estimated with likelihood function.

Nucleus	^{100}Mo	^{82}Se	Best limits from previuos experiments	
			^{100}Mo	^{82}Se
$n = 1$	$> 2.7 \cdot 10^{22}$	$> 1.5 \cdot 10^{22}$	$> 5.8 \cdot 10^{21}$ [52]	$> 2.4 \cdot 10^{21}$ [40]
$n = 2$	$> 1.7 \cdot 10^{22}$	$> 6.0 \cdot 10^{21}$	$> 3.0 \cdot 10^{20}$ [53]	$> 1 \cdot 10^{21}$ [53]
$n = 3$	$> 1.0 \cdot 10^{22}$	$> 3.1 \cdot 10^{21}$	$1.6 \cdot 10^{20}$ [40]	$6.3 \cdot 10^{20}$ [40]
$n = 7$	$> 7 \cdot 10^{19}$	$> 5.0 \cdot 10^{20}$	$4.1 \cdot 10^{19}$ [40]	$1.1 \cdot 10^{19}$ [40]

Table 4

The QRPA nuclear matrix elements for ^{100}Mo and ^{82}Se.

Nucleus	$M_F - M_{GT}$	M_{CR}	$M_{F\omega^2} - M_{GT\omega^2}$
^{82}Se	2.63-5.60 [27,28,29]	0.14-0.44 [39,55]	10^{-3} [39]
^{100}Mo	2.97-5.37 [27,28,29]	0.16-0.44 [39,55]	10^{-3} [39]

Table 5

Phase-space integrals (G [y $^{-1}$]) for different nuclei and models of decay (from [54] for n = 1 and from [39] for n = 3,7.)

Nucleus	$2\beta\chi^0$, $n=1$	$2\beta\chi^0$, $n=3$	$2\beta\chi^0\chi^0$,$n=3$	$2\beta\chi^0\chi^0$, $n=7$
^{82}Se	$4.84 \cdot 10^{-16}$	$3.49 \cdot 10^{-18}$	$1.01 \cdot 10^{-17}$	$7.73 \cdot 10^{-17}$
^{100}Mo	$8.23 \cdot 10^{-16}$	$7.28 \cdot 10^{-18}$	$1.85 \cdot 10^{-17}$	$1.54 \cdot 10^{-16}$

Table 6

Limits on the Majoron coupling constant $\langle g_{ee} \rangle$ at the 90% CL for ^{100}Mo and ^{82}Se.

model	mode	n	^{82}Se	^{100}Mo
IB	$2\beta\chi^0$	1	$(0.66 - 1.7) \cdot 10^{-4}$	$(0.4 - 1.8) \cdot 10^{-4}$
IC	$2\beta\chi^0$	1	$(0.66 - 1.7) \cdot 10^{-4}$	$(0.4 - 1.8) \cdot 10^{-4}$
IIB	$2\beta\chi^0$	1	$(0.66 - 1.7) \cdot 10^{-4}$	$(0.4 - 1.8) \cdot 10^{-4}$
ID	$2\beta\chi^0\chi^0$	3	2.4	1.5
IE	$2\beta\chi^0\chi^0$	3	2.4	1.5
IIC	$2\beta\chi^0$	3	0.022-0.068	0.0088-0.024
IID	$2\beta\chi^0\chi^0$	3	2.4	1.5
IIF	$2\beta\chi^0$	3	0.022-0.068	0.0088-0.024
IIE	$2\beta\chi^0\chi^0$	7	1.3	3.2